



# Experimental studies of Portevin-Le Chatelier plastic instabilities in carbon-manganese steels by infrared pyrometry

N. Ranc<sup>a,\*</sup>, W. Du<sup>b</sup>, I. Ranc<sup>b</sup>, D. Wagner<sup>b</sup>

<sup>a</sup> PIMM, UMR CNRS 8106, Arts et Métiers-ParisTech, 151 Boulevard de l'Hôpital, 75013 Paris, France

<sup>b</sup> Université Paris Ouest Nanterre, LEME, 50 rue de Sèvres, 92410 Ville d'Avray, France

## ARTICLE INFO

### Article history:

Received 20 November 2015

Received in revised form

17 February 2016

Accepted 21 March 2016

Available online 22 March 2016

### Keywords:

Portevin-Le Chatelier bands

Carbon-manganese steel

Dynamic strain aging

Infrared thermography

## ABSTRACT

The dynamic strain aging (DSA) phenomenon that occurs in some materials under certain temperature and strain rate conditions can cause plastic strain localization in the form of Portevin-Le Chatelier (PLC) bands. Carbon-manganese steels are used commonly and frequently in construction because of their ductility, low cost and ability to form mechanically. In these steels, the DSA phenomenon occurs for common quasi-static strain rates from 150 to 300 °C, which makes band observation complicated. PLC bands on a carbon-manganese steel that was sensitive to DSA were studied using an infrared camera. Specimen heating was achieved using an induction furnace (with an adapted coil inductor), which allows for temperature recording during tensile tests. Thermography with an infrared camera was used to estimate the band characteristics and increments in band plastic strain, which is an important parameter for material behavior identification necessary for DSA phenomenon modeling. This technique had been developed only for PLC phenomenon observation at ambient temperature on aluminum alloys. Band characteristics on the carbon-manganese steels have been compared with results obtained previously on aluminum alloys.

© 2016 Elsevier B.V. All rights reserved.

## 1. Introduction

Carbon-manganese (C-Mn) steels are common steels that are used frequently in construction because of their ductility, low cost and ability to form mechanically. The metallurgy of these steels is complex, because of the interaction of solute atoms with dislocations during deformation, which leads to metallurgical instabilities, which include Lüders strain, static strain aging (SSA) and dynamic strain aging (DSA). If these metallurgical instabilities induce an increase in hardness, they produce a decrease in ductility that is detrimental to component safety [1–10].

Lüders strain appears at the transition between elastic and plastic domains from 20 to 200 °C. At the upper yield stress, the stress drops suddenly; plastic deformation begins at one side of the specimen and propagates as a plastic front through the length of the sample. SSA occurs if unloading is conducted during homogeneous plastic deformation, followed by heat treatment at 200 °C over a few minutes and reloading. This results in a return of the Lüders strain phenomenon. These phenomena (Lüders and SSA) are visible at room temperature. Thereafter, plastic deformation is homogeneous during the

test until area reduction occurs.

In DSA, aging is sufficiently rapid to occur during straining. Strain localization is characterized in a tensile test by the formation and propagation of plastic strain bands termed Portevin-Le Chatelier (PLC) bands. During tensile tests at an imposed strain rate, DSA is associated with serrations on the stress-strain curve [4,11–16]. Each stress drop on the tensile curve corresponds to the formation of a band. Three types of bands form: type A corresponds to the continuous propagation of a plastic front along the specimen, type B corresponds to a discontinuous but regular propagation of bands and type C corresponds to chaotic formation along the specimen (discontinuous and uncorrelated). At a microscopic scale, this phenomenon is related to the interaction of mobile dislocations with the interstitial solute atoms. Dislocation gliding is discontinuous [17–21], and the dislocations are stopped temporarily on the obstacles (forest, precipitates) during a waiting time  $t_w$ . During this waiting time, solute atom diffusion creates additional anchoring of dislocations. This anchoring effect is active in a strain rate and temperature domain. In C-Mn steels, the DSA phenomenon occurs for common quasi-static strain rates for 150–300 °C, which complicates observations [9,10].

In C-Mn steels, carbon and nitrogen atoms interact with dislocations. Because of its greater solubility limit, nitrogen seems to influence aging more than carbon does [1,5,22,23]. The location of these atoms is rather complex [9,10]. One part is precipitated as

\* Corresponding author.

E-mail address: [nicolas.ranc@ensam.eu](mailto:nicolas.ranc@ensam.eu) (N. Ranc).

<sup>1</sup> <http://pimm.paris.ensam.fr/fr/user/9>.

carbides ( $\text{Fe}_3\text{C}$ ) or nitrides ( $\text{Fe}_4\text{N}$ ,  $\text{Fe}_{16}\text{N}_2$  or aluminum nitride if aluminum is present). The other part is in solid solution in the centered cubic iron lattice. The part in solid solution is distributed in three locations [24–26]. Most of the atoms gather and form “Cottrell atmospheres”. Some segregate near dislocations in the interstitial sites and, when all sites near the dislocations are occupied, the remaining solute atoms are free in the lattice interstitial sites. It appears that solute atoms in “Cottrell atmospheres” cause SSA and thus the Lüders phenomenon. Moreover, it has been demonstrated that in C-Mn steels, free carbon and nitrogen in the interstitial sites are responsible for DSA [27]. Recently, literature models and C-Mn steels have been reviewed by [28,29].

PLC band observation on aluminum alloys has been studied extensively. In this case, DSA occurs at room temperature. The techniques used are optical extensometry [30–33], speckle interferometry [34–39], digital image correlation [40–44] or thermography with an infrared camera [45–48]. The advantage of this latter technique is that increments of plastic strain in the bands can be estimated. This is an important parameter that is useful for material behavior identification and is necessary for DSA phenomenon modeling. However, this technique has only been developed for the PLC phenomenon at ambient temperature.

In this study, infrared thermography has been used at 200 °C, which is the operating temperature for DSA in C-Mn steels. Specimen heating was achieved using an induction furnace (with an adapted coil inductor), which allows for temperature recording during the tensile tests. After the study material has been presented, the experimental techniques are described and the experimental results (band characteristics) are presented and compared with aluminum alloy results in literature.

## 2. Experimental setup

### 2.1. Material

C-Mn was received as a 40-mm-thick plate. Its chemical composition (weight percent) is reported in Table 1. The plate was treated by prior normalization thermal treatment, which included austenitizing at 900 °C followed by furnace cooling (to 300 °C) and air cooling. This leads to a microstructure that is composed of banded ferrite and pearlite.

This material contains too little aluminum (0.0085%) to allow for full precipitation of nitrogen atoms by aluminum nitride formation during cooling from the austenitic region. Consequently, after this heat treatment, some free nitrogen still exists in the lattice, which makes this alloy sensitive to DSA.

### 2.2. Loading device and specimen

Tensile tests were carried out using a hydraulic tensile machine. Grip displacement was controlled to obtain a constant velocity. Two grip velocities were considered. The nominal tensile strain was deduced from the measurement of grip displacements and the tensile stress was measured using a force sensor. Specimen geometry is given in Fig. 1. The specimen was placed at the center of the inductor of an induction furnace, and its temperature was controlled to ensure that it remained constant at the specimen center. Temperature control time was shorter than the required for PLC band formation.

**Table 1**  
Composition of C-Mn steel.

	C	N	Mn	Al
Weight %	0.190	1.07	0.011	0.0085

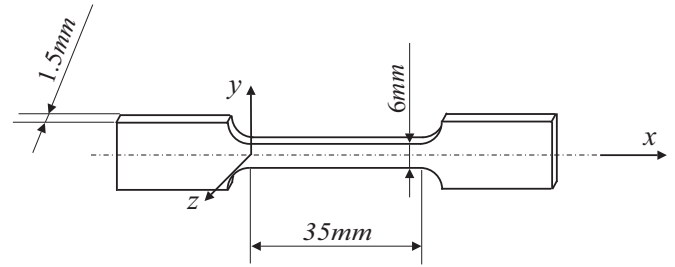


**Fig. 1.** Tensile test specimen geometry.

Table 2 lists the nominal strain rate and mean temperature for various tests.

### 2.3. PLC band observation technique

As mentioned previously, various techniques have been used to study PLC bands and to quantify their parameters (bandwidth, apparent propagation velocity, increase in plastic deformation in the band). We have used an infrared thermography measurement technique that was developed 10 years ago [45,46]. This technique has been used in many previous studies on PLC at ambient temperature [45–57]. One advantage of this technique is that it allows for the estimation of band parameters and for a following of their evolution during the entire tensile test. In this paper, infrared thermography has been adapted to the study of PLC phenomena at higher temperature and in particular, for the study of C-Mn steels.

The principle of this technique is based on a measure of the temperature field on the specimen surface induced by plastic energy dissipated in heat during band formation. The links between plastic strain in the band and the temperature field measured is given by a heat transfer equation. A homogeneous temperature can be assumed for flat specimens of small thickness, and the heat transfer equation is written as:

$$\rho C \frac{\partial T}{\partial t} = \sigma : \dot{\epsilon}_p + k \left( \frac{\partial^2 T}{\partial x^2} + \frac{\partial^2 T}{\partial y^2} \right) - \frac{2h}{e} (T - T_{amb}) \quad (1)$$

where  $\rho$  is the density,  $C$  is the heat capacity per unit mass,  $k$  is the thermal conductivity,  $h$  is the convection coefficient,  $e$  is the specimen thickness and  $T_{amb}$  is the ambient temperature. The first term on the right-hand side represents the heat source associated with dissipated plastic energy, where  $\sigma$  and  $\epsilon$  are the stress and strain tensors, respectively. It is supposed here that the plastic energy is dissipated completely as heat. The second term represents heat transfer from heat conduction. This term is a priori not equal to zero as soon as the temperature field remains heterogeneous. The last term of Eq. (1) corresponds to thermal losses by convection and radiation on the specimen surface.

If losses are neglected, i.e., convection, radiation and conduction terms are neglected compared with thermal inertia, the heat equation can be simplified and is given after time integration:

$$\rho C \Delta T = \sigma : \Delta \epsilon_p. \quad (2)$$

Under these conditions, a proportionality relation exists between the temperature variation  $\Delta T$  and the increment in plastic strain  $\Delta \epsilon_p$ . This adiabatic assumption is valid as soon as temperature increments are measured over short times. For example, this case exists when the variation in temperature as measured between two images taken by the camera and the frequencies of acquisition are sufficiently large. In this paper, this adiabatic assumption will always be made and associated errors from thermal losses on estimated parameters will be quantified.

An infrared charge-coupled device camera was used to measure temperature variation fields associated with the dissipation of

Download English Version:

<https://daneshyari.com/en/article/7975483>

Download Persian Version:

<https://daneshyari.com/article/7975483>

[Daneshyari.com](https://daneshyari.com)